A Wireless Pressure-Measurement System Using a SAW Hybrid Sensor

Gernot Schimetta, *Member, IEEE*, Franz Dollinger, and Robert Weigel, *Senior Member, IEEE*

***Abstract*—A pressure-measurement system based on surface-acoustic-wave (SAW) sensors is presented in this paper. Since SAW sensors are powered by the energy of the RF field, no battery is required, which is a major drawback of conventional microcontroller-based telemetry systems. A successful combination of a SAW reflective delay line with a high-Q capacitive pressure sensor is shown. With a new way of matching the sensor impedance to the SAW reflector impedance, both a high signal-to-noise ratio and a high signal dynamic are achieved, which supports accurate signal evaluation. As an example of realization, the prototype of a tire pressure sensor unit is presented.**

***Index Terms*—Pressure measurement, surface-acoustic-wave delay lines, telemetry.**

I. Introduction

THE development of a "smart tire," capable of continuously transmitting information about its actual state, is a technical challenge for automotive research groups worldwide. Especially monitoring the pressure and temperature inside car and truck tires is becoming increasingly important. The aim is both to prevent accidents caused by a tire burst and to provide an economical advantage through a reduction of fuel consumption and a longer tire lifetime. The measurement of the actual tire parameters is based on the application of a wireless sensor system. In general, three different technologies may be used for wireless information transmission [1]: radio transmission including an active sensor unit, radio transmission by reflection (passive transponder), and inductive transmission. In the case of tire pressure measurement, the application of inductive transmission drops out due to the low distance that would be required between the coil mounted in the wheel arch and the coil inside the tire.

In the past, several systems consisting of an active battery-powered sensor unit inside each wheel and a central receiver unit have been realized [2], [3]. The major problem of these microcontroller-based systems is the required lithium battery, which limits the lifetime of the sensor unit. In this paper, a different approach based on radio transmission by reflection is presented. Here, surface-acoustic-wave (SAW) devices are implemented as passive transponders. Wireless passive SAW sensors for several physical quantities have been developed over the last decade [4], [5]. Main features of SAW sensor systems are a large readout distance and an energy supply of the sensor only by the electromagnetic RF field of the transceiver unit. Consequently, in the case of tire pressure measurement, a high inquiry rate does not decrease the lifetime of the sensor unit and enables the detection of a sudden pressure decrease inside the tire.

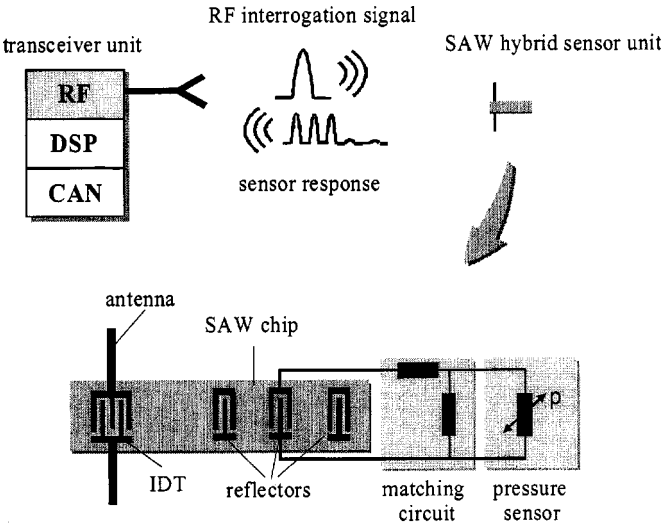

Fig. 1. Schematic drawing of a SAW sensor system applied to pressure measurement.

This paper describes the design of a tire pressure-measurement system using SAW transponders. After a short characterization of the measurement system, the sensor unit and its components, a prototype of the tire pressure sensor unit, is presented. Measurement results are reported and discussed.

II. SAW Sensor System

In Fig. 1, a schematic drawing of the tire pressure-measurement system as an example of a wireless SAW hybrid sensor system is shown. A measurement cycle is initiated by a high-frequency electromagnetic burst signal ($f_0 = 433.92$ MHz) emitted from a central transceiver unit. This signal is received by the antenna of the SAW transponder unit mounted on the rim. The interdigital transducer (IDT) connected to the antenna transforms the received signal into a SAW. All of the acoustic reflectors placed within the acoustic path of the SAW reflect parts of the incoming wave. The first and third reflector in Fig. 1 are used as reference, whereas the second one is electrically connected to a pressure sensor. In the IDT, the reflected acoustic waves are reconverted into an electromagnetic pulse train and retransmitted to the central transceiver unit, where the received signal is amplified, down converted, and analyzed.

In Fig. 2, the block diagram of the transceiver unit is shown. As can be seen, the architecture is similar to that of an impulse

Manuscript received March 2, 2000; revised August 25, 2000.

G. Schimetta is with the Institute for Communications and Information Engineering, Johannes Kepler University of Linz, A-4040 Linz, Austria.

F. Dollinger is with Siemens, D-81730 Munich, Germany.

R. Weigel is with the Institute for Communications and Information Engineering, University of Linz, A-4040 Linz, Austria.

Publisher Item Identifier S 0018-9480(00)10753-7.

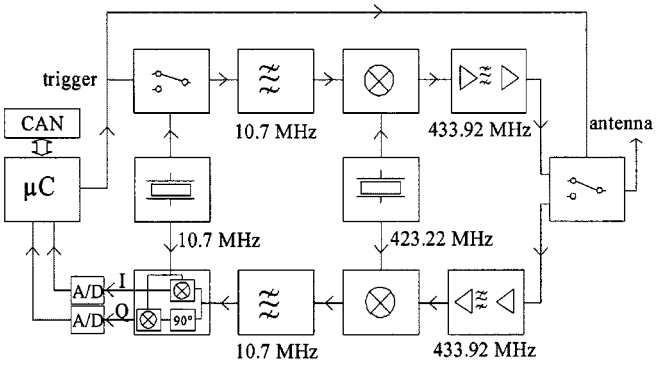

Fig. 2. Schematic drawing of a transceiver unit employed in the SAW pressure sensor system.

radar. The transmitted burst signal is created by switching an intermediate-frequency continuous-wave signal, where the switch is triggered by a microcontroller. The generated 10.7-MHz burst signal is filtered and mixed with 423.22 MHz. The resulting amplified burst meets the specifications of the 433.92-MHz industrial–scientific–medical (ISM) channel. After the transmission of the inquiry burst signal, the transceiver unit is switched into receiving mode. The incoming signal is amplified by a low-noise amplifier (LNA), down converted to the intermediate frequency and filtered. After all, it is demodulated in the quadrature demodulator unit. With the digitized I and Q signals, a microcontroller is supplied. The microcontroller itself is equipped with a controller area network (CAN) interface and is responsible for the calculation of the sensor data and providing it to automotive safety and stability systems.

The raw sensor data include both information on the propagation characteristic of the SAW and the reflection properties of the acoustic reflectors. Since the velocity of the SAW depends on temperature, the tire temperature can be determined by measuring the time delay between the two reflected pulses of the reference reflectors in Fig. 1. The low propagation velocity of the SAW allows a long delay time between the RF interrogation signal and sensor response. Additionally, in the case of a reflective delay line, the acoustic path on the piezoelectric substrate (e.g., lithium–niobate) is used twice, also resulting in very small SAW chips. Particular attention has to be paid to the transmission path between the central transceiver and sensor units. Due to the fact that the RF interrogation signal has to cover twice the distance between the transceiver and sensor units without amplification along the way, the attenuation is doubled compared to conventional battery-powered sensor systems. Thus, the signal amplitude received by the transceiver unit is several orders lower than the amplitude of the emitted interrogation signal.

Nevertheless, using the ISM frequency band at 433.92-MHz interrogation distances of 1–2.5 m are feasible, which enables the implementation as a tire-pressure sensor system [5]. Since a single interrogation cycle takes only about 20 μs, even sensor units mounted on fast moving or rotating parts can read out successfully.

III. Impedance-Loaded SAW Delay Line

In former SAW pressure sensor designs [6], [7], the reflective delay line was both used as transponder and sensor. The SAW delay line was embedded into a piezoelectric diaphragm with a hermetically closed cavity beneath. Bending under the applied pressure, some of the diaphragm sections were compressed and some were stretched. The phase velocity of the SAW is slower in stretched sections, whereas it is faster in compressed sections. Thus, the pressure sensor information was included in the time delay between the pulses generated by the acoustic reflectors of the delay line.

With reference to the demands of the automotive industry, a smaller pressure sensor unit at lower costs was desired. A solution was found in the application of a reflective delay line of which one acoustic reflector is electrically loaded with the impedance of an "external" pressure sensor [9]. The three acoustic reflectors, shown in Fig. 1, are implemented as splitfinger IDTs. The second IDT is terminated with a matching circuit and the sensor impedance (Z_{sensor}), which varies with the measurand. In (1), the reflectivity of an impedance-loaded reflector as a function of the matched sensor impedance is represented by the complex scattering parameter S_{11}

$$S_{11}(Z_{\mathrm{sensor}}) = \frac{2P_{13}^2}{P_{33} + \dfrac{1}{Z_{\mathrm{sensor}} + Z_{\mathrm{match}}}}. \qquad (1)$$

The parameters P_{13} and P_{33} in (1) are elements of the P-matrix, which describes the electroacoustic coupling of a single IDT with two acoustical ports (indexes 1 and 2) and one electrical ports (index 3). Thus, the electroacoustic parameter P_{13} specifies the relation between the amplitude of the outgoing acoustic wave and the amplitude of the voltage at port 3 of the IDT. Therefore, $(P_{13})^2$ represents the electroacoustical power transmission of the IDT. P_{33} equals the electrical admittance of the IDT [10].

Since the sensor impedance modulates the reflected pulse both in amplitude and phase, there are two ways of calculating the sensor information in the time domain. One strategy is to match the sensor impedance to the electrical impedance of the reflector in the way that the amplitude modulation is maximized [9]. This is outlined in Fig. 3, where the amplitude of the reflected pulse as a function of the load impedance is shown as a "contour line" in a Smith chart. The simulation is based on the scattering parameters of a realized reflective SAW delay line measured by a network analyzer. Simulations based on the application of (1) lead to the same results.

As can be seen in Fig. 3, a very high impedance variability is needed to modulate the magnitude of S_{11} between the maximum and minimum of reflectivity. In the case of reactive sensors, a high-Q factor of the sensor impedance is also needed. With the help of a matching circuit, the sensor impedance range can be transformed to the region in the Smith chart, where a high reflectivity can be observed. Although a change of more than 20 dB in the reflectivity could be achieved with realized sensors [9], there is a drawback in deriving the sensor information from the amplitude of the reflected pulses. Since the attained amplitude resolution depends on the actual signal-to-noise ratio, the usable range in Fig. 3 and, thus, the achievable readout distance, is limited.

To overcome this limitation, we present a new way of matching, which is shown for the first time in this paper. Following this, the sensor impedance is adapted to the acoustic

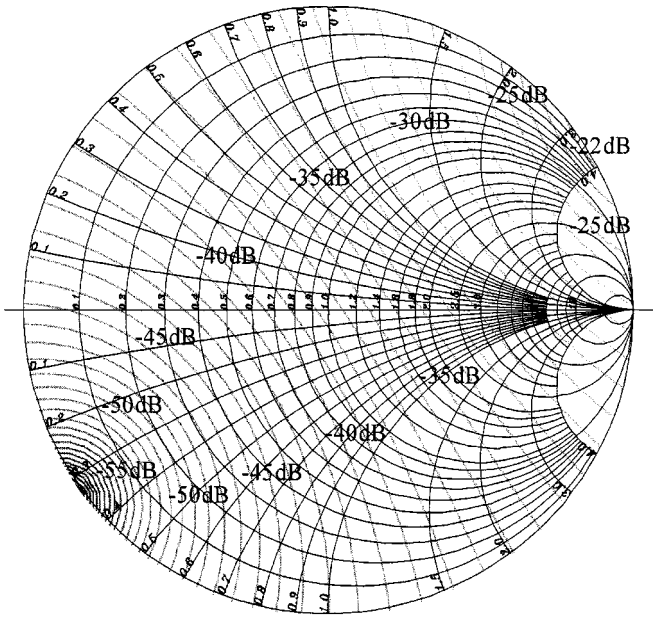

Fig. 3. Impedance load-dependent amplitude $|S_{11}|$ of the reflected pulse. Points of constant reflectivity are interconnected.

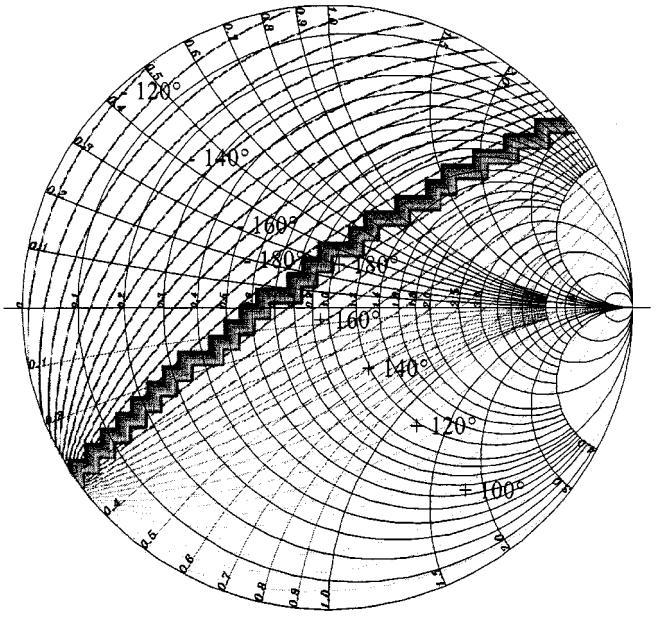

Fig. 4. Phase φ_{S11} of the reflected pulse as a function of the electrical load impedance. Points of constant reflectivity are interconnected.

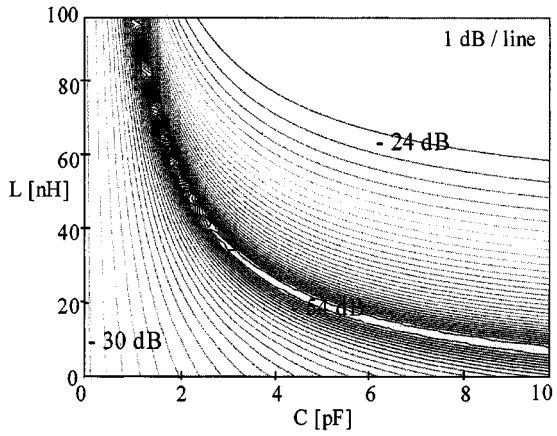

Fig. 5. Magnitude of the scattering parameter S_{11} representing the reflectivity of an impedance-loaded reflective delay line as a function of the variable sensor capacitance and serial inductance of a matching coil. Points of constant reflectivity are interconnected.

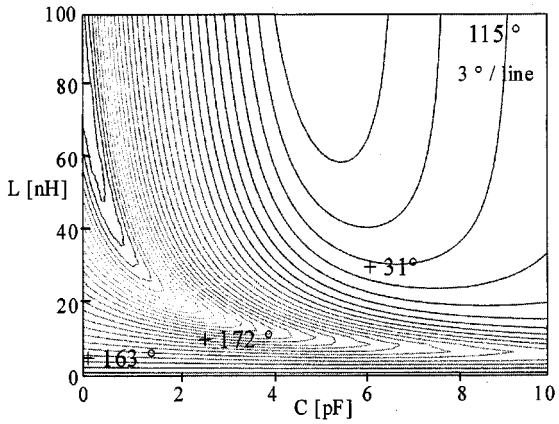

Fig. 6. Phase difference $\Delta\varphi_{S11}$ between two reflected pulses of a delay line as a function of the variable sensor capacitance and serial inductance of a matching coil connected to one acoustic reflector. Points of constant reflectivity are interconnected.

reflector in the way that the phase modulation is maximized. In Fig. 4, the phase φ_{S11} of the reflected pulse is shown as a function of the load impedance. The orthogonality between the contour plots in Figs. 3 and 4 is due to the fact that phase and amplitude are linked by the Hilbert transformation [11]. Since both a high signal-to-noise ratio and a high phase-modulation factor is desirable, the appropriate matching can be found by comparing Figs. 3 to 4. The influence of the RF transmission path can be eliminated by using the phase difference $\Delta\varphi_{S11}$ between the pulses of the loaded reflector and a reference reflector for the calculation of the pressure.

In order to simplify the determination of the appropriate matching, the magnitude of the reflected pulse is shown as a function of matched sensor impedance in Fig. 5. The respective phase difference $\Delta\varphi_{S11}$ between the reflected pulses of the electrically loaded reflector and one reference reflector is shown as a function of the matched sensor impedance in Fig. 6. Both diagrams are based on the assumption of a variable sensor capacitance and a constant series resistance of 5 Ω, a typical value of realized sensors. The sensor impedance is matched to the impedance of the splitfinger IDT with the help of a lossless series coil.

The same diagrams can also be used for sensors with a measurand dependent inductance. In that case, the sensor impedance has to be matched to the impedance of the connected acoustic reflector with the help of an appropriate capacitance. Simulations of a parallel inductance matching or a matching based on combinations of several inductances lead to similar diagrams, as shown in Figs. 5 and 6. Basically, the applicability of an impedance sensor as load for a SAW delay line depends on the Q factor of the impedance. A low-Q factor dramatically reduces both the achievable magnitude and phase modulation. Nevertheless, with limitations, resistive impedance sensors with a very

high resistance span can also be applied as an impedance load [9].

With respect to tire pressure measurement, the knowledge of the temperature inside the tire is also necessary to evaluate the measured pressure data. As mentioned before, the temperature can be determined by measuring the time delay between the two reflected pulses of the reference reflectors due to the temperature dependence of the SAW propagation. Generally, a change in the environmental temperature $\Delta\vartheta$ results in a variation of the acoustic path length Δl and a variation of the SAW phase velocity Δv. Thus, the propagation time τ along the acoustic path of the reflective SAW delay line changes [5]

$$\frac{\Delta\tau}{\tau} = \left(\frac{\Delta l}{l\Delta\vartheta} - \frac{\Delta v}{v\Delta\vartheta}\right)\Delta\vartheta = TCD_1\Delta\vartheta. \tag{2}$$

In (2), TCD_1 represents the first-order temperature coefficient of delay. In the case of a YZ–lithium–niobate ($LiNbO_3$) substrate, which we used for the SAW reflective delay line, the temperature coefficient of delay is 94 ppm/K [12], where the first-order thermal expansion coefficients are $\alpha_{11} = \alpha_{22} = 15.4$ ppm/K [13]. With common transceiver units, a temperature resolution of typically ± 1 K can be achieved by measuring the time delay between two pulses generated by reference reflectors. Nevertheless, customary SAW temperature-measurement systems operate with deriving the temperature from the phase difference $\Delta\varphi$ between two reflected pulses resulting in a temperature resolution of ± 0.02 K [5]. The phase difference $\Delta\varphi$ caused by a change of delay time $\Delta\tau$ also depends on the used carrier frequency f_0

$$\Delta\varphi = 2\pi f_0\Delta\tau. \tag{3}$$

In case of impedance-loaded reflective delay lines, the phase shift caused by thermal variation usually exceeds the phase shift of the varying impedance load. A solution was found in arranging the electrically loaded reflector equidistant between two reference reflectors, as shown in Fig. 1. The sensor information is then calculated from the phase difference between the measured phase of the loaded reflector and the average value of both phases generated by the reference reflectors. In that way, the thermal-dependent phase shifts due to varying time delays between the reference reflector and electrically loaded reflector are eliminated. Assuming a phase shift caused by the electric load of less than 180°, no phase ambiguity occurs. The successful implementation of the new way of matching leading to a maximum of phase modulation, and the results of calculating the sensor information from the received phase signal are shown in Section V.

IV. Sensor Unit Prototype

A. Capacitive Pressure Sensor

Although it is generally possible to adapt both inductive and capacitive sensors to the reflector of the SAW delay line, using capacitive sensors is more advantageous because a lower series resistance and temperature coefficient and a good reproducibility at low price can be achieved.

Silicon-based surface and bulk micromachined capacitive pressure sensors found on the market were investigated, but showed poor suitability for the application due to their low-Q factor. The measured low-Q factor can be explained by the fact that the electrodes of micromachined capacitive pressure sensors based on silicon technology are usually structured by doping the silicon, which results in a rather high serial resistance (about 20–50 Ω). An ultrahigh doping of the silicon membrane leading to higher Q factors would impair the mechanical properties of the diaphragm. Therefore, a new high-Q capacitive differential pressure sensor composed of two quartz structures having minimal thermal stress and a low-temperature coefficient [7] was designed. A prototype of the sensor and its components is shown in Fig. 7. In the quartz cover plate, a quadratic blind hole was structured with the help of a sandblast apparatus. On the resulting diaphragm, a common electrode with an electrically isolating cover layer was deposited. On the other quartz plate, two electrodes with a layer thickness of 1-μm aluminum were structured. Both parts were joined with a one-component epoxy adhesive at atmospheric pressure, forming a hermetically sealed cavity. The geometry of the sensor was determined by the use of a finite-element method (FEM) program.

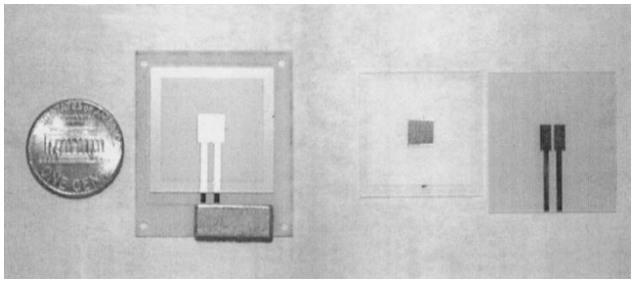

Fig. 7. High-Q capacitive differential pressure sensor prototype and its components.

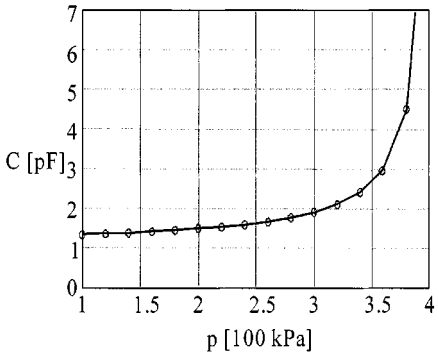

Fig. 8. Measured capacitance of the differential pressure sensor as a function of the applied pressure.

The sensor was designed for a pressure range of 100 up to 400 kPa, an excess pressure stability of 600 kPa, and a heat stability up to 130 °C. In Fig. 8, the measured capacitance as a function of the applied pressure is shown. Comparing the sensor capacitance curve to the diagrams in Figs. 5 and 6, the appropriate matching circuit was determined to be a 100-nH series inductance. The membrane electrode of the sensor touches the bottom electrodes above the regular pressure range. Since the membrane electrode is coated with an isolation layer, this "touch-down" range can also be utilized for measurements. The

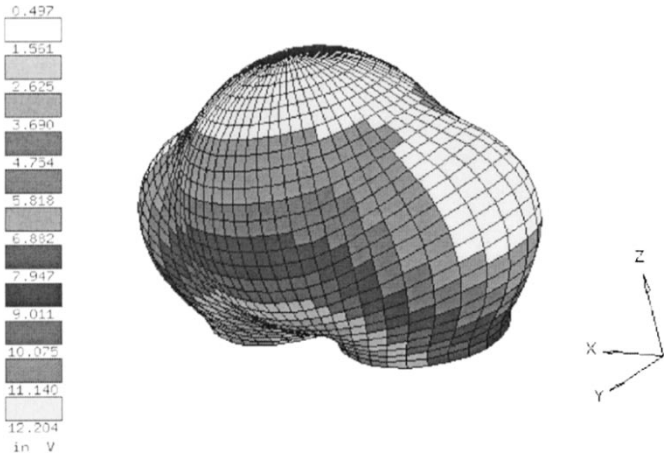

Fig. 9. Simulated directional diagram for the short-range field (distance: 30 cm) of the realized rim antenna. The antenna is fed with a power of 30 dBm. In order to simplify the calculation, the rim is assumed to be a conductive plane. The antenna is arranged along the x-axis.

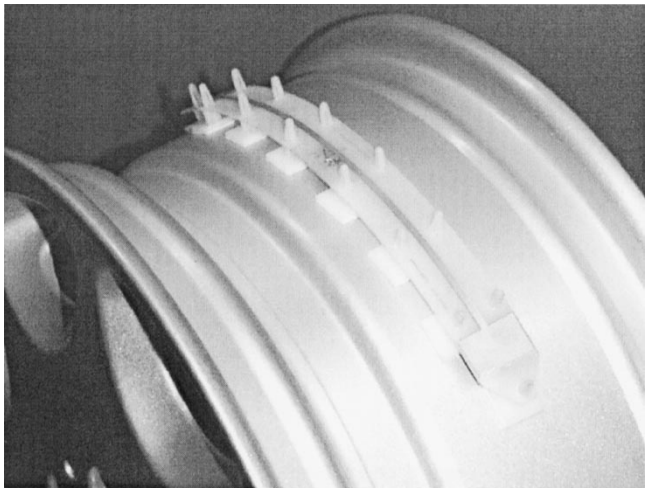

Fig. 10. Prototype of a capacitively shortened dipole antenna mounted on a rim. The antenna is etched out of the copper layer of a 0.5-mm FR-4 substrate. The SAW hybrid pressure sensor is mounted on the backside of the plate.

relatively high layer thickness of the electrodes and the low resistivity of aluminum results in a measured series resistance of only about 3 Ω.

B. Rim Antenna

Transmittance measurements at car tires showed a one-way attenuation of about −20 dB at 434 MHz. Especially the transmittance through the steel belt of the tire lead to high losses. An alternative way was found in using the tire sidewall for transmission. Several types of antennas were simulated. In Fig. 9, the simulated directional diagram of a capacitively shortened $\lambda/2$ dipole antenna, which seemed most suitable for the application as rim antenna, is shown. In order to simplify the simulation, the diameter of the rim was assumed to be infinite. The well-known antenna gain of a $\lambda/2$ dipole ($G = 2.1$ dB) can be enhanced by mounting the dipole on the conductive rim with an appropriate distance. In Fig. 10, the first prototype of the dipole antenna is shown. The antenna substrate represents also the carrier for the SAW delay line, matching circuit, and pressure sensor. All of them are mounted on the backside and are covered with a protective silicone layer. With the help of capacitive shortening, the length of the antenna could be reduced to $l = 24$ cm.

V. Measurement Results

In Fig. 11, the measured phase difference $\Delta\varphi_{S11}$ and the signal insertion loss $|S_{11}|$ of the SAW hybrid pressure sensor unit are shown as functions of the tire pressure. Herein, the losses of the transmission path are not included. As can be seen, a phase modulation of 110° at a low-signal-level dependency on the varying pressure was obtained. Compared to conventional pressure sensors, it is remarkable that the pressure resolution is not constant within the whole pressure range. Both the maximum insertion loss of −32 dB and the insertion loss variation of 8 dB are very low compared to conventional hybrid SAW sensors optimized with respect to amplitude modulation.

In combination with a $\lambda/2$ dipole antenna mounted in the wheel arch and a transceiver unit described in Section II, a typical signal-to-noise ratio of 20 dB was measured. As a result, a typical accuracy better than ±15 kPa is achievable. When turning the wheel, one single maximum of signal level without multipath distortion was measured.

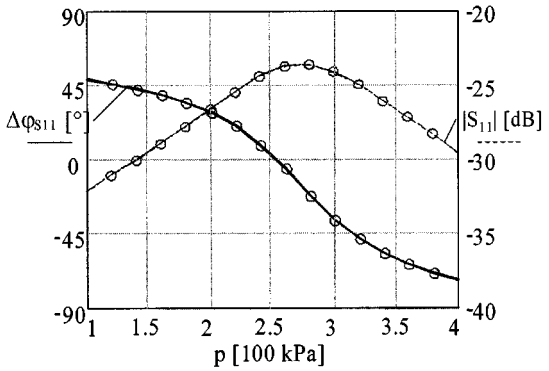

Fig. 11. Measured phase difference $\Delta\varphi_{S11}$ and amplitude $|S_{11}|$ of the reflected pulse as functions of the tire pressure.

As a further step, an optimization of the transmission path between sensor and transceiver units including the wheel arch antenna and a miniaturization of the capacitive pressure sensor will be undertaken. As a final step, it is planned to integrate the sensor unit into the tire valve.

VI. Conclusion

The principle and design of a pressure-measurement system based on the combination of a SAW transponder tag with a high-Q capacitive pressure sensor to a SAW hybrid sensor has been presented in this paper. A new way of matching the sensor impedance with the reflective SAW delay line leading to both a high signal-to-noise ratio and a high modulation factor was introduced. The prototype of a tire pressure sensor unit with a typical accuracy of ±15 kPa within a pressure range of 100–400 kPa, an excess pressure stability of 600 kPa, and a heat stability up to 130 °C has also been presented.

ACKNOWLEDGMENT

The authors would like to thank W.-E. Bulst, Corporate Department of Technology, Siemens, Munich, Germany, and G. Scholl, Corporate Department of Technology, Siemens, Munich, Germany, for continuous encouragement, C. Korden, Corporate Department of Technology, Siemens, Munich, Germany, for valuable advice regarding the antenna design and B. Bienert, Corporate Department of Technology, Siemens, Munich, Germany, S. Berek, Corporate Department of Technology, Siemens, Munich, Germany, K. Riek, Corporate Department of Technology, Siemens, Munich, Germany, and H. Zottl, Corporate Department of Technology, Siemens, Munich, Germany, for the fabrication and assembly of the SAW devices.

REFERENCES

[1] H. Wunderlich, G. Hettich, M. Klein, R. Schraub, and J. Schenk, "Concepts and steps in the development of wireless sensors and actuators for automotive applications," in *Proc. Sensor'99*, vol. 2, Nuremberg, Germany, pp. 157–162.

[2] B. De Geeter, O. Nys, M. Chevroulet, and J.-P. Bardyn, "A wireless tire pressure and temperature monitoring system," in *Proc. Sens. Expo. Conf.*, 1996, pp. 61–63.

[3] J. Lee, H. Kulka, and J. Schramm, "Transponder and sensor apparatus for sensing and transmitting vehicle tire parameter data," U.S. Patent US5 731 754, Mar. 24, 1998.

[4] F. Seifert, W. E. Bulst, and C. Ruppel, "Mechanical sensors based on surface acoustic waves," *Sens. Actuators A, Phys.*, vol. 44, pp. 231–239, 1994.

[5] G. Scholl, F. Schmidt, T. Ostertag, L. Reindl, H. Scherr, and U. Wolff, "Wireless passive SAW sensor systems for industrial and domestic applications," in *Proc. IEEE Freq. Control Symp.*, 1998, pp. 595–601.

[6] L. Reindl, G. Scholl, T. Ostertag, H. Scherr, U. Wolff, and F. Schmidt, "Theory and application of passive SAW radio transponders as sensors," *IEEE Trans. Ultrason., Ferroelect., Freq. Contr.*, vol. 45, pp. 1281–1292, Sept. 1998.

[7] H. Scherr, G. Scholl, F. Seifert, and R. Weigel, "Quartz pressure sensor based on SAW reflective delay line," in *IEEE Proc. Freq. Contr. Symp.*, 1996, pp. 347–350.

[8] A. Pohl and F. Seifert, "Wirelessly interrogable surface acoustic wave sensors for vehicular applications," *IEEE Trans. Instrum. Meas.*, vol. 46, pp. 1031–1038, Aug. 1997.

[9] R. Steindl, A. Pohl, and F. Seifert, "Impedance loaded SAW-sensors offer a wide range of measurement opportunities," *IEEE Trans. Microwave Theory Tech.*, vol. 47, pp. 2625–2629, Dec. 1999.

[10] G. Tobolka, "Mixed matrix representation of SAW-transducers," *IEEE Trans. Sonic Ultrason.*, vol. SU-26, pp. 426–428, Nov. 1979.

[11] D. P. Morgan, *Surface Wave Devices for Signal Processing*. Amsterdam, The Netherlands: Elsevier, 1985, p. 92f, 199f.

[12] D. P. Morgan, "SAW's on lithium niobate: Properties of common orientations," in *Properties of Lithium Niobate*, ser. EMIS Datareviews 5. New York: Inspec, 1989, pp. 84–93.

[13] R. Smith and F. Welsh, "Temperature dependence of the elastic, piezoelectric, and dielectric constants of lithium tantalate and lithium niobate," *J. Appl. Phys.*, vol. 42, no. 6, pp. 2219–2230, 1971.

[14] G. Montress, T. Parker, and J. Callerame, "A miniature hybrid circuit SAW oscillator using an all quartz packaged resonator," in *Proc. IEEE Ultrason. Symp.*, 1985, pp. 277–282.

Gernot Schimetta (S'96–M'98) was born in Linz, Austria, in 1971. He received the Master's degree in electrical engineering from the University of Technology, Graz, Austria, in 1997, and is currently working toward the Ph.D. degree at the Johannes Kepler University of Linz, Linz, Austria.

He is currently with the Johannes Kepler University of Linz, where his responsibilities include the design of wireless SAW sensor systems. He has also been involved with common research activities with the Siemens Corporate Research Center, Munich, Germany.

Franz Dollinger was born in Augsburg, Germany, in 1965. He received the electrical engineering degree in technical electrophysics and the Ph.D. degree from the Technical University of Munich, Munich, Germany, in 1991 and 1996, respectively. His doctoral research concerned the ultrafast directional coupler switches for optical data transmission.

He is currently with Siemens, Munich, Germany. Since 1997, he has been involved with wireless sensor systems based on SAW devices. His main activities are focused on temperature sensors and automotive applications.

Robert Weigel (S'88–M'89–SM'95) was born in Ebermannstadt, Germany, in 1956. He received the Dr.-Ing. and Dr.-Ing.habil. degrees in electrical engineering and computer science from the Munich University of Technology, Munich, Germany, in 1989 and 1992, respectively.

While with the Munich University of Technology, he has been a Research Engineer (1982–1988), a Senior Research Engineer (1988–1994), and a Professor for RF circuits and systems (1994–1996). In the winter of 1994–1995, he was a Guest Professor of SAW technology at the Vienna University of Technology, Vienna, Austria. Since 1996, he has been the Director of the Institute for Communications and Information Engineering at the University of Linz, Linz, Austria. Since 1998, he has also been a Professor of RF engineering at Tongji University, Shanghai, China. He has been engaged in research and development on microwave theory and techniques, integrated optics, high-temperature superconductivity, SAW technology, and digital and microwave communication systems. In these fields, he has authored or co–authored over 200 papers and has given over 120 international presentations. His review work includes European research projects and international journals. In August 1999, he co-founded Danube Integrated Circuit Engineering (DICE), Linz, Austria, an Infineon Technologies company, which is devoted to the design of mobile radio circuits and systems.

Dr. Weigel is a member of the Institute for Components and Systems of The Electromagnetics Academy and a member of the German Informationstechnieche Gesellschaft (ITG) and the Austrian Engineering Society (ÖVE). In 1993, he was the corecipient of the Microwaves and Optronics (MIOP) Award.